Hindawi
Journal of Metallurgy
Volume 2019, Article ID 1678431, 1 page
https://doi.org/10.1155/2019/1678431

Retraction

Retracted: Inhibition Effect of Substituted Thiadiazoles on Corrosion Activity of N80 Steel in HCl Solution

Journal of Metallurgy

Received 13 November 2018; Accepted 13 November 2018; Published 10 March 2019

Journal of Metallurgy has retracted the article titled "Inhibition Effect of Substituted Thiadiazoles on Corrosion Activity of N80 Steel in HCl Solution" [1]. The article was found to contain images reused in several other articles published by Mahendra Yadav and colleagues. The details of the reuse of images are as follows:

Figure 9(b) is similar to Figure 11b in [2], Figure 17b in [3], Figure 14b in [4], and Figure 5b in [5]. Figure 9(c) is similar to Figure 11c in [2], Figure 17c in [3], and Figure 14c in [4]. In particular, Figure 9 in [1] shares the same image of a sample in HCl as Figure 11 in [2] and the same image in the presence of an inhibitor, but these represent different inhibitors in each article, AMPT, and BAL, respectively.

We asked the authors to provide the underlying uncropped and unadjusted scanning electron microscopy (SEM) images, the raw data, and details of how the experiments were conducted.

The corresponding author, Dr. Yadav, said the SEM work was outsourced but did not give details on where, when, or by whom this work was performed. The equipment is described as a "JEOL JSM-6380 LA analytical scanning electron microscope" in this article. However, there is no description of the scanning electron microscope in [2] and in [6] it is described as a "Scanning Electron Microscope model SEM Jeol JSM-5800." These are not the same model of microscope, despite these articles sharing some of the same SEM images.

Dr. Yadav provided us with replacement figures. However, they were identical for two of the articles, [1, 6], despite representing experiments with the inhibitors AMPT and ODAEODI, respectively. We were not told how these images were generated, the images were of low resolution, and the text in the images was illegible.

The corresponding author agreed to retraction and we have asked the institution to formally investigate.

References

[1] M. Yadav, S. Kumar, and D. Behera, "Inhibition Effect of Substituted Thiadiazoles on Corrosion Activity of N80 Steel in HCl Solution," *Journal of Metallurgy*, vol. 2013, Article ID 256403, 14 pages, 2013.

[2] M. Yadav, S. Kumar, and P. N. Yadav, "Corrosion Inhibition of Tubing Steel during Acidization of Oil and Gas Wells," *Journal of Petroleum Engineering*, vol. 2013, Article ID 354630, 9 pages, 2013.

[3] M. Yadav, U. Sharma, and P. N. Yadav, "Isatin compounds as corrosion inhibitors for N80 steel in 15% HCl," *Egyptian Journal of Petroleum*, vol. 22, no. 3, pp. 335–344, 2013.

[4] M. Yadav, U. Sharma, and P. Yadav, "Corrosion inhibitive properties of some new isatin derivatives on corrosion of N80 steel in 15% HCl," *International Journal of Industrial Chemistry*, vol. 4, no. 1, p. 6, 2013.

[5] M. Yadav, P. N. Yadav, and U. Sharma, "Substituted imidazoles as corrosion inhibitors for N80 steel in hydrochloric acid," *Indian Journal of Chemical Technology*, vol. 20, pp. 363–370, 2013.

[6] M. Yadav, S. Kumar, U. Sharma, and P. N. Yadav, "Substituted amines as corrosion inhibitors for N80 steel in 15%HCl," *Journal of Materials and Environmental Science*, vol. 4, no. 5, pp. 691–700, 2013.

Hindawi Publishing Corporation
Journal of Metallurgy
Volume 2013, Article ID 256403, 14 pages
http://dx.doi.org/10.1155/2013/256403

Research Article

Inhibition Effect of Substituted Thiadiazoles on Corrosion Activity of N80 Steel in HCl Solution

M. Yadav, Sumit Kumar, and Debasis Behera

Department of Applied Chemistry, Indian School of Mines, Dhanbad 826004, India

Correspondence should be addressed to M. Yadav; yadav_drmahendra@yahoo.co.in

Received 29 November 2012; Revised 2 March 2013; Accepted 18 March 2013

Academic Editor: Elena V. Pereloma

The inhibition effect of some prepared compounds, namely, thiadiazole derivatives, on N80 steel corrosion in 15% HCl solutions has been studied by using the weight loss, electrochemical polarization, and electrochemical impedance spectroscopy techniques. It was found that the inhibition efficiency of the thiadiazole derivatives, namely, 2-amino-5-(4-methoxyphenyl)-1,3,4-thiazole (AMPT), 2-amino-5-phenyl-1,3,4-thiazole (APT), and 2-amino-5-(4-chlorophenyl)-1,3,4-thiazole (ACPT), increases with the increase in concentration. Inhibition efficiency follows the order AMPT > APT > ACPT. The effect of temperature on the corrosion was investigated by the weight loss method, and some thermodynamic parameters were calculated. The inhibitive action may be attributed to the adsorption of inhibitor molecules on the active sites of the metal surface following Langmuir adsorption isotherm. Polarization measurements indicated that thiadiazole derivatives act as mixed-type corrosion inhibitor. The adsorption of thiadiazole derivatives on N80 surface exposed to inhibitor-containing solutions was confirmed using SEM and FT-IR spectra.

1. Introduction

N80 carbon steel has been generally used as the main construction material for down hole tubular, flow lines, and transmission pipelines in petroleum industry. In most industrial processes, acidic solutions are commonly used for pickling, industrial acid cleaning, acid descaling, oil well acidifying, and so forth [1–5]. It is commonly noticed that 15–28% of hydrochloric acid is used for the acidization of petroleum oil wells [6, 7]. Because of their aggressiveness, iron and its alloys get corrodes during these acidic applications particularly with the use of hydrochloric acid and sulphuric acid, which results in terrible waste of both resources and money [8]. Addition of inhibitor remains the necessary procedure to secure the metal against acid attack. Therefore, corrosion inhibitors for HCl solutions have attracted more attention. Most of the well-known corrosion inhibitors are organic compounds containing polar groups having nitrogen, sulphur, and/or oxygen atoms and heterocyclic compounds with polar functional groups and conjugated double bonds [9, 10]. These compounds can adsorb on the metal surface and partially blocking the active sites on the surface, thereby reducing the corrosion rate. Among different nitrogen- and sulphur-containing compounds, thiosemicarbazide has been reported to be a potential inhibitor for different metals [11, 12]. Most of the investigation is related to the application of common inhibitors like various derivatives of the compound of aminothiazoles [13], benzotriazoles [14–16], thioimidazole [17], mercapto-5-triazole [18], and thiadiazole [19, 20] which have been used as potential inhibitors for this system.

Keeping in the view of the above excellent behavior of the organic compounds containing nitrogen and sulphur as corrosion inhibitors, some compounds of substituted thiadiazoles, namely, 2-amino-5-(4-methoxyphenyl)-1, 3,4-thiadiazole (AMPT), 2-amino-5-phenyl-1,3,4-thiadiazole (APT), and 2-amino-5-(4-chlorophenyl)-1,3,4-thiadiazole (ACPT), have been synthesized, and their corrosion inhibition property was studied by the weight loss technique and electrochemical techniques.

2. Experimental Section

2.1. Materials

2.1.1. Composition of N80 Sample. The working electrode and specimens for weight loss experiments were prepared from oil

well N80 steel having the percentage composition (wt.%) as shown in Table 1. The specimens were mechanically abraded with 320, 400, 600, 800, 1000, and 1200 emery paper, washed in acetone and double-distilled water, then dried, and put into the cell.

2.1.2. Solutions. The aggressive solutions were made up of 37% HCl (Rankem). The concentration of the used inhibitors ranged from 20 ppm to 200 ppm in 15% HCl. All solutions were prepared in double-distilled water.

2.1.3. Synthesis of Corrosion Inhibitor. The inhibitors AMPT, APT, and ACPT were synthesized in the laboratory by a reported method [21] as shown in Scheme 1. An equimolar mixture of substituted benzoic acid (0.05 mol), thiosemicarbazide (0.05 mol), and phosphorous oxychloride (15 mL) was refluxed gently for half an hour. After cooling, water was added (45 mL) and the mixture was refluxed for 4 h and filtered. The solution was neutralized with saturated solution of potassium hydroxide. The precipitate was filtered and recrystallized from ethanol. Their purity was confirmed by TLC. The structure of inhibitors is shown in Table 2.

2.2. Methods

2.2.1. Weight Loss Method. The N80 specimens were cut in the dimension of 3 cm × 3 cm × 0.1 cm with a small hole of 2 mm at the upper edge of specimen for weight loss studies, and the size of the electrodes was 1 cm × 1 cm with 4 cm long tag for electrochemical studies with an exposed area of 1 cm^2 towards aggressive solution. The specimens were mechanically abraded successively with 1/0, 2/0, 3/0, and 4/0 grade emery papers. The surface was thoroughly washed with soap, running tap water, and distilled water and finally was degreased with acetone. The samples were dried and stored in vacuum desiccators before immersion in the test solution. Weight loss measurements were performed at 303 K for 6 h by immersing the N80 steel coupons into 250 mL of 15% hydrochloric acid in the absence and the presence of various amounts of inhibitors. After the elapsed time, the specimens were taken out, washed, dried, and weighed accurately. The experimental studies were performed at temperature range of 303 K to 333 K. The inhibition efficiency (IE%) and surface coverage (θ) were determined by using following equation [22]:

$$\mathrm{CR}\,(\mathrm{mmpy}) = \frac{87.6\Delta W}{DAT}, \tag{1}$$

where ΔW = weight loss (mg), D = density of specimen (g/cm^3), A = area of specimen (cm^2), and T = exposure time (hours). The degree of surface coverage (θ) by inhibitors can be expressed in terms of corrosion rate as

$$\theta = \frac{\mathrm{CR}_0 - \mathrm{CR}_{\mathrm{inh}}}{\mathrm{CR}_0}, \qquad \mathrm{IE\%} = \frac{\mathrm{CR}_0 - \mathrm{CR}_{\mathrm{inh}}}{\mathrm{CR}_0} \times 100, \tag{2}$$

Table 1: Composition of specimens.

C	Mn	Si	P	S	Cr	Fe
0.31	0.92	0.19	0.01	0.008	0.20	Remainder

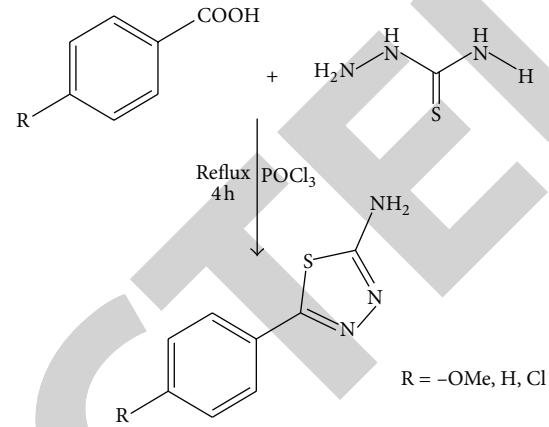

Scheme 1

where CR_0 = corrosion rate in the absence of inhibitor and $\mathrm{CR}_{\mathrm{inh}}$ = corrosion rate in the presence of inhibitor.

2.2.2. Electrochemical Method. The electrochemical experiments were carried out in a three-necked glass assembly containing 250 mL of the electrolyte with different concentrations of inhibitors (from 20 ppm to 200 ppm by weight) dissolved in it. The electrochemical studies were carried out with N80 steel strips having an exposed area of 1 cm^2. The rest of the samples were isolated from the working environment by a cold mounting process, for which epoxy resin had been used. A conventional three-electrode cell consisting of N80 steel as a working electrode, platinum as counter electrode, and a saturated calomel electrode as reference electrode was used. Polarisation studies were carried out using an AMEL Potentiostat 2053, Italy, connected to a personal computer. Prior to electrochemical measurements, the working electrode was first immersed into the test solution for 30 min to establish a steady-state open circuit potential. After the establishment of the open circuit potential, dynamic polarization curves were obtained with a scan rate of 1 mV/s in the potential range from −470 to −390 mV with scan rate of 10 m Vs^{-1}. All potentials were measured against SCE. All experiments were performed at 30 ± 0.2°C in an electronically controlled air thermostat. The inhibition efficiency (IE %) was calculated using the following equation:

$$\%\ \mathrm{IE} = \left[\frac{(I_0 - I_{\mathrm{inh}})}{I_0}\right] \times 100, \tag{3}$$

where I_0 = corrosion current in the absence of inhibitor and I_{ihn} = corrosion current in the presence of inhibitor.

AC-impedance studies were carried out in three-electrode cell assembly containing N80 steel as the working electrode, platinum as counter electrode, and saturated calomel as reference electrode. The impedance measurements

Table 2: Name and structural formulae of compounds thiadiazole derivatives.

Compound	Structure	Name and abbreviation
1	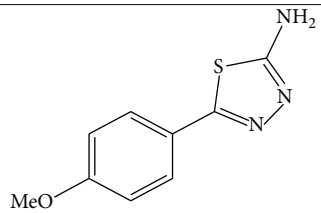	2-Amino-5-(4-methoxyphenyl)-1,3,4-thiadiazole (AMPT)
2	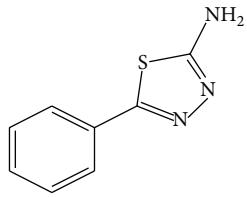	2-Amino-5-phenyl-1,3,4-thiadiazole (APT)
3	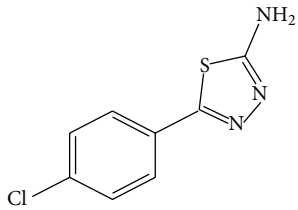	2-Amino-5-(4-chlorophenyl)-1,3,4-thiadiazole (ACPT)

were carried out at an open circuit potential (OCP), after 30 min immersion of the N80 steel electrode in the corrosive medium. The impedance data were acquired in the frequency range of 100 KHz–50 mHz with an AC voltage amplitude of 10 mV. The charge transfer resistance (R_{ct}) and double-layer capacitance (C_{dl}) were determined from Nyquist plots. The inhibition efficiencies were calculated from charge transfer resistance values by using the following formula:

$$\% \text{ IE} = \left[\frac{R_{ct(inh)} - R_{ct}}{R_{ct(inh)}}\right] \times 100, \quad (4)$$

where R_{ct} = charge transfer resistance in absence of inhibitor; $R_{ct(Inh)}$ = charge transfer resistance in presence of inhibitor.

2.2.3. Scanning Electron Microscopic (SEM) Analysis. The N80 specimens of size 1.0 cm × 1.0 cm × 0.06 cm were abraded with a series of emery papers (grades 320, 500, 800, and 1200) and then washed with distilled water and acetone. After immersion in 15% HCl in the absence and the presence of optimum concentration of inhibitor (AMPT) at 30°C for 6 h, the specimen was cleaned with distilled water, dried with a cold air blaster, and then the SEM images were recorded using JEOL JSM-6380 LA analytical scanning electron microscope.

2.2.4. FT-IR Spectroscopy. For the FTIR studies the N80 steel coupons were immersed in 15% HCl containing optimum concentration of inhibitors (AMPT, APT, and ACPT) for 24 h. The test coupons were then removed from the solution, washed thoroughly with distilled water and dried. The film formed on the N80 surface in the presence of the inhibitor was collected by nonmetallic scrapper from the surface of the steel for spectral analysis with Fourier transform infrared spectroscopy (FT-IR). FT-IR spectra were recorded between 4000 cm^{-1} and 400 cm^{-1}, and the scraped films were recorded using a Perkin Elmer Model 2000, by KBr pellet method.

Table 3: The variation of percentage inhibition efficiency obtained from weight loss studies.

Concentration (ppm)	(IE percent) inhibition efficiency		
	AMPT	APT	ACPT
20	63.27	60.32	57.32
50	67.72	64.51	60.65
100	74.84	70.45	67.47
150	80.27	77.58	73.51
200	82.32	79.03	75.71

3. Results and Discussion

3.1. Weight Loss Measurement. Corrosion inhibition efficiency (IE%) offered by inhibitors (AMPT, APT, and ACPT) has been evaluated by weight loss technique after 6 h of immersion at 303 K which is given in Table 3. From this table it is apparent that inhibition efficiency (IE%) was increased with the increase in the concentration of the inhibitor [23]. The maximum of 82.3% inhibition efficiency was obtained at the 200 ppm inhibitor (AMPT) concentration. No considerable effect on the inhibition efficiency (IE%) was observed by a further increase in the inhibitor concentration in the acid solution. From this table, the order of the inhibition efficiency follows the order AMPT > APT > ACPT. Corrosion inhibition studies were also carried out at different temperatures.

Table 4: Corrosion parameters, namely, corrosion rate (CR), surface coverage (θ), and inhibition efficiency IE (%) of N80 steel in 15% HCl in the presence and the absence of the inhibitor at different temperatures, obtained from weight loss measurements.

Inhibitor	Conc (ppm)	303 K			313 K			323 K			333 K		
		CR (mmpy)	θ	IE%	CR (mmpy)	θ	IE%	CR (mmpy)	θ	IE%	CR (mmpy)	θ	IE%
Blank	—	2.672	—	—	9.084	—	—	17.943	—	—	60.348	—	—
AMPT	20	0.983	0.632	63.2	2.906	0.680	68.0	4.719	0.737	73.7	14.00	0.768	76.8
	50	0.863	0.677	67.7	2.416	0.734	73.4	3.893	0.783	78.3	10.00	0.833	83.3
	100	0.673	0.748	74.8	1.607	0.823	82.3	2.440	0.864	86.4	6.155	0.898	89.8
	150	0.529	0.802	80.2	1.317	0.855	85.5	1.920	0.893	89.3	5.129	0.915	91.5
	200	0.446	0.823	82.3	1.090	0.880	88.0	1.596	0.911	91.1	4.586	0.924	92.4
APT	20	1.060	0.603	60.3	3.148	0.653	65.3	5.678	0.683	68.3	16.66	0.724	72.4
	50	0.948	0.645	64.5	2.831	0.688	68.8	4.670	0.739	73.9	12.69	0.789	78.9
	100	0.790	0.704	70.4	2.128	0.766	76.6	3.583	0.800	80.0	9.975	0.839	83.9
	150	0.600	0.775	77.5	1.769	0.805	80.5	3.019	0.832	83.2	8.189	0.864	86.4
	200	0.552	0.793	79.3	1.349	0.851	85.1	2.486	0.861	86.1	6.914	0.894	89.4
ACPT	20	1.140	0.573	57.3	3.455	0.619	61.9	6.263	0.651	65.1	19.60	0.675	67.5
	50	1.053	0.606	60.6	3.332	0.633	63.3	5.363	0.701	70.1	14.83	0.754	75.4
	100	0.869	0.674	67.4	2.503	0.725	72.5	4.419	0.754	75.4	12.40	0.794	79.4
	150	0.708	0.735	73.5	2.082	0.770	77.0	3.676	0.795	79.5	10.72	0.822	82.2
	200	0.649	0.757	75.7	1.637	0.819	81.9	3.136	0.825	82.5	8.762	0.855	85.5

Corrosion parameters, namely, corrosion rate (CR), surface coverage (θ), and inhibition efficiency (IE %) of N80 steel in 15% HCl in the presence and absence of inhibitor at different temperature, obtained from weight loss measurements, are shown in Table 4. As shown from this table, by increasing the concentration of the inhibitor, corrosion rate decreases; as a result, the inhibition efficiency was increased with rise in temperature [24]. For all concentrations of AMPT, the systems at 333 K gave the highest efficiencies. The maximum efficiency of 92% was obtained for 200 ppm AMPT at 333 K. The variation in corrosion rate with different concentration of thiadiazole derivatives in 15% HCl at different temperature is shown in Figure 1. It is evident from Figure 1 that the inhibitor (AMPT, APT, and ACPT) has shown remarkable corrosion inhibition at a higher temperature. The variation of inhibition efficiency with the temperature is shown in Figure 2. From this figure, order of the inhibition efficiency of thiadiazole derivatives is as follows: AMPT > APT > ACPT. High efficiency of these compounds was attributed to the presence of extensively delocalized π electrons of the phenyl rings, planarity, and the presence of lone pair of electrons on N and S atoms which favored a greater adsorption of inhibitors on the metal surface [25].

3.1.1. Thermodynamic and Activation Parameters. Thermodynamic and activation parameters play important role in understanding the inhibitive mechanism. The weight loss measurements were done in the temperature range of 303–333 K in the absence and the presence of different concentrations of inhibitors (AMPT, APT, and ACPT) in 15% HCl for N80 steel. The apparent activation energy (E_a) for dissolution of N80 steel in 15% HCl can be expressed using the Arrhenius equation,

$$\log \mathrm{CR} = \frac{-E_a}{2.303RT} + \log A, \tag{5}$$

Table 5: Activation parameter for N80 in 15% HCl solution in the absence and the presence of the inhibitor obtained from weight loss measurements.

Inhibitor	Concentration (ppm)	E_a (kJ mol^{-1})	ΔH^* (kJ mol^{-1})	ΔS^* (Jmol^{-1} K^{-1})
Blank	—	85.06	84.14	40.99
AMPT	20	72.93	66.09	−26.78
	50	66.67	64.75	−32.29
	100	60.32	62.80	−40.62
	150	62.32	59.13	−54.68
	200	63.78	49.40	−88.48
APT	20	75.40	71.61	−8.63
	50	70.50	66.87	−24.38
	100	70.15	65.50	−30.71
	150	72.25	67.63	−25.73
	200	69.41	66.00	−32.34
ACPT	20	78.53	71.73	−6.60
	50	72.64	68.45	−18.37
	100	72.66	68.72	−19.13
	150	74.13	69.77	−17.30
	200	71.15	69.44	−20.50

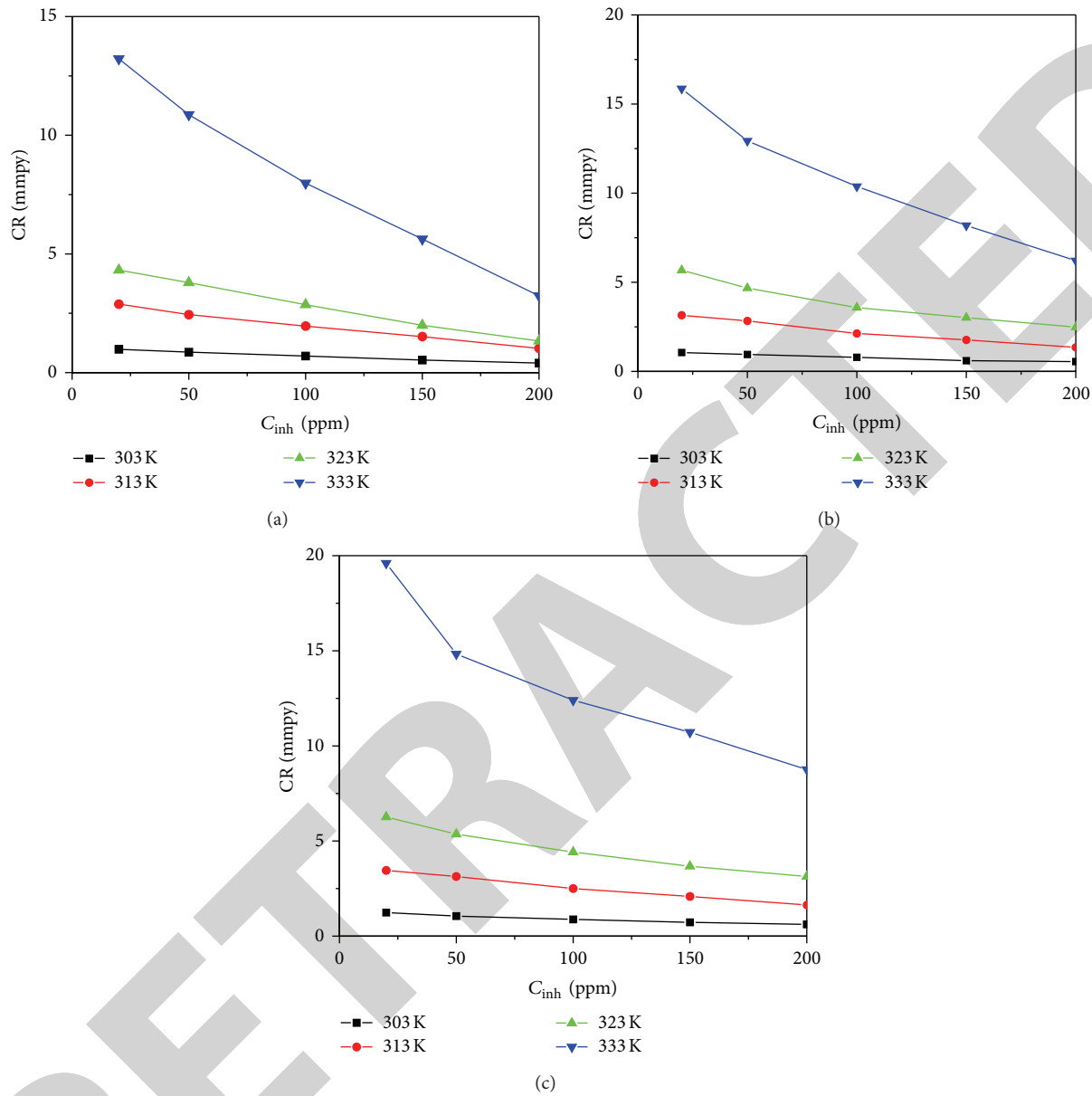

Figure 1: A plot of corrosion rate versus inhibitor's concentrations at different temperatures. (a) AMPT, (b) APT, and (c) ACPT.

where CR is the corrosion rate, E_a is the apparent activation energy, R is the molar gas constant ($8.314\,\mathrm{J\,K^{-1}\,mol^{-1}}$), T is the absolute temperature, and A is the Arrhenius pre-exponential factor. Figure 3 represents the Arrhenius plot of log CR against $1/T$ for the corrosion of N80 steel in 15% HCl solution with or without the presence of AMPT, APT, and ACPT at concentrations ranging from 20 ppm to 200 ppm. From Figure 3, the slope ($-E_a/R$) of each individual line was determined, and the activation energy has been calculated by using (E_a = (slope) × 2.303 × R) and the values of E_a were summarized in Table 5. It is evident from Table 5 that the decrease in activation energy E_a indicates the retardation in corrosion rate which could have occurred because of the adsorption of the inhibitors at the surface of the metal [26].

The value of enthalpy of activation of the ΔH^* and the entropy of activation ΔS^* can be calculated by using the following formula:

$$\mathrm{CR} = \frac{RT}{Nh}\exp\left(\frac{\Delta S^*}{R}\right)\exp\left(-\frac{\Delta H^*}{RT}\right), \qquad (6)$$

where CR is the corrosion rate, H^* is the enthalpy of activation, S^* is the entropy of activation, h is Planck's constant, and N is the Avogadro number, respectively.

A plot of log (CR/T) against $1/T$ (Figure 4) gave straight lines with slope of ($-\Delta H^*/2.303R$) and intercept of (log $R/Nh + \Delta S^*/2.303R$) from which the activation thermodynamic parameters (ΔH^* and ΔS^*) are estimated and listed in Table 5. The results which are presented in Table 5 show that

Table 6: Electrochemical parameter and percentage inhibition efficiency obtained from polarisation studies for N80 steel in 15% HCl solution in the presence or the absence of the inhibitors at 303 K.

Inhibitor	Concentration (ppm)	E_{corr} (mV_{SCE})	b_a (mV dec^{-1})	b_c (mV dec^{-1})	I_{corr} ($\mu A\ cm^{-2}$)	% IE
Blank	—	−427	95	135	573	
AMPT	20	−434	55	104	178	68.87
	50	−437	64	82	160	72.02
	100	−438	77	93	134	76.54
	150	−445	157	142	95	83.37
	200	−447	111	128	80	86.51
APT	20	−428	74	147	203	64.52
	50	−432	61	73	182	68.21
	100	−433	53	84	154	73.21
	150	−436	92	98	106	81.58
	200	−438	108	44	103	82.03
ACPT	20	−430	68	102	229	60.02
	50	−431	75	91	205	64.05
	100	−432	88	79	177	69.07
	150	−434	97	108	133	76.81
	200	−436	118	156	114	80.07

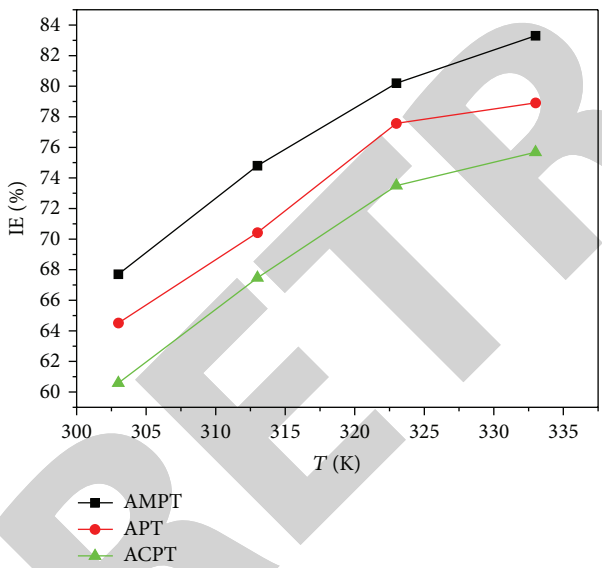

Figure 2: Variation of inhibition efficiency of the studied compounds with the temperature containing optimum concentration of inhibitor.

the enthalpy of activation is all positive. The positive sign of the enthalpy reflects the endothermic nature of the N80 steel dissolution process [27]. The negative value of ΔS^* (Table 5) for all the three inhibitors indicates that activated complex in the rate determining step represents an association rather than a dissociation step, meaning that a decrease in disorder takes place during the course of transition from the reactant to the activated complex, and the positive value of ΔS^* refers to an increase in the disorder [28].

3.2. Potentiodynamic Polarization Measurements. The anodic and cathodic polarisation curves for the corrosion of N80 steel in 15% HCl in the presence and the absence of varying concentrations of inhibitors (AMPT, APT, and ACPT) at 303 K are shown in Figure 6. The linear Tafel segments of the cathodic and anodic curves were extrapolated to the point of intersection to obtain the corrosion potential (E_{corr}) and corrosion current density (i_{corr}). The electrochemical parameters such as corrosion potential (E_{corr}), corrosion current density (i_{corr}), anodic (b_a) and cathodic (b_c) Tafel slope, and percentage inhibition efficiency (IE%) determined from polarisation curve are summarized in Table 6. The data in Table 6 clearly show that the current density decreases with the presence of thiadiazole inhibitors (AMPT, APT, and ACPT); this indicated that inhibitors adsorbed on the metal surface, and hence the inhibition efficiency increases with the increase in the inhibitor concentration up to an optimum value. Thereafter, the increase in the inhibitor concentration resulted in negligible increase in inhibition efficiency and the presence of inhibitor caused small changes in (E_{corr}) value. This implies that the inhibitor acts as a mixed-type inhibitor, affecting both anodic and cathodic reactions [29]. According to Li et al. [30], if the displacement in E_{corr} is more than ±85 mV/SCE relating to E (corrosion potential of the blank), the inhibitor can be considered as a cathodic or anodic type. If the change in E_{corr} is less than 85 mV, the corrosion inhibitor may be regarded as a mixed type. But the maximum displacement in the present case is less than 20 mV/SCE, which indicates that AMPT, APT, and ACPT act as mixed-type inhibitors. It is concluded that the inhibitor's molecules retard the corrosion process without changing the mechanism of corrosion process in the medium of investigation. However, the shift of E_{corr} values towards positive direction on increasing the concentration

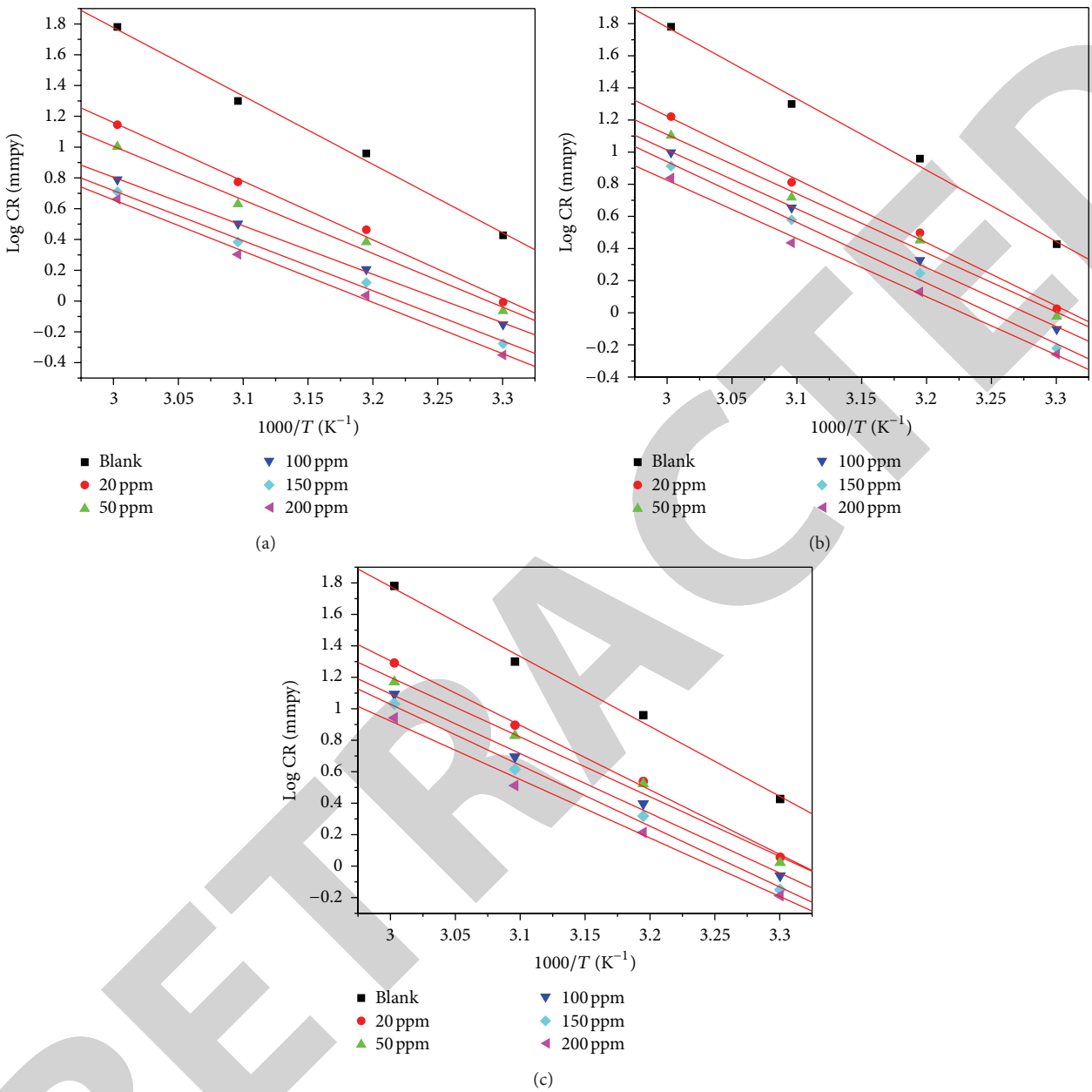

Figure 3: Arrhenius plots of log CR versus 1000/T for N80 steel corrosion in 15% HCl (a) AMPT, (b) APT, and (c) ACPT.

of thiadiazole derivatives suggests anodic control over the reaction.

3.3. Electrochemical Impedance Spectroscopy (EIS). Nyquist plots of N80 steel in 15% HCl solution in the absence and the presence of different concentrations of AMPT, APT, and ACPT at 303 K are shown in Figures 7(a), 7(b), and 7(c). It follows from Figures 7(a), 7(b), and 7(c) that a high frequency (HF) depressed charge-transfer semicircle was observed. The experimental data obtained from these plots are fitted by the equivalent electrical circuit shown in Figure 8. Such an equivalent circuit was also discussed by several researchers, who obtained similar depressed semicircles with single time constant due to surface heterogeneity of corrosion product covering the surface at random sites [31–33]. The charge-transfer resistance (R_{ct}) values were calculated from the difference in impedance at low and high frequencies. The values of electrochemical double-layer capacitance (C_{dl}) were calculated at the frequency f_{max}, at which the imaginary component of the impedance is maximal ($-Z_i$) by the following equation:

$$C_{dl} = \frac{1}{2\pi f_{max} R_{ct}}. \quad (7)$$

The constant phase element of double-layer (CPE) is mathematically expressed as

$$Z_{CPE} = Y_0^{-1} (i)^{-n}, \quad (8)$$

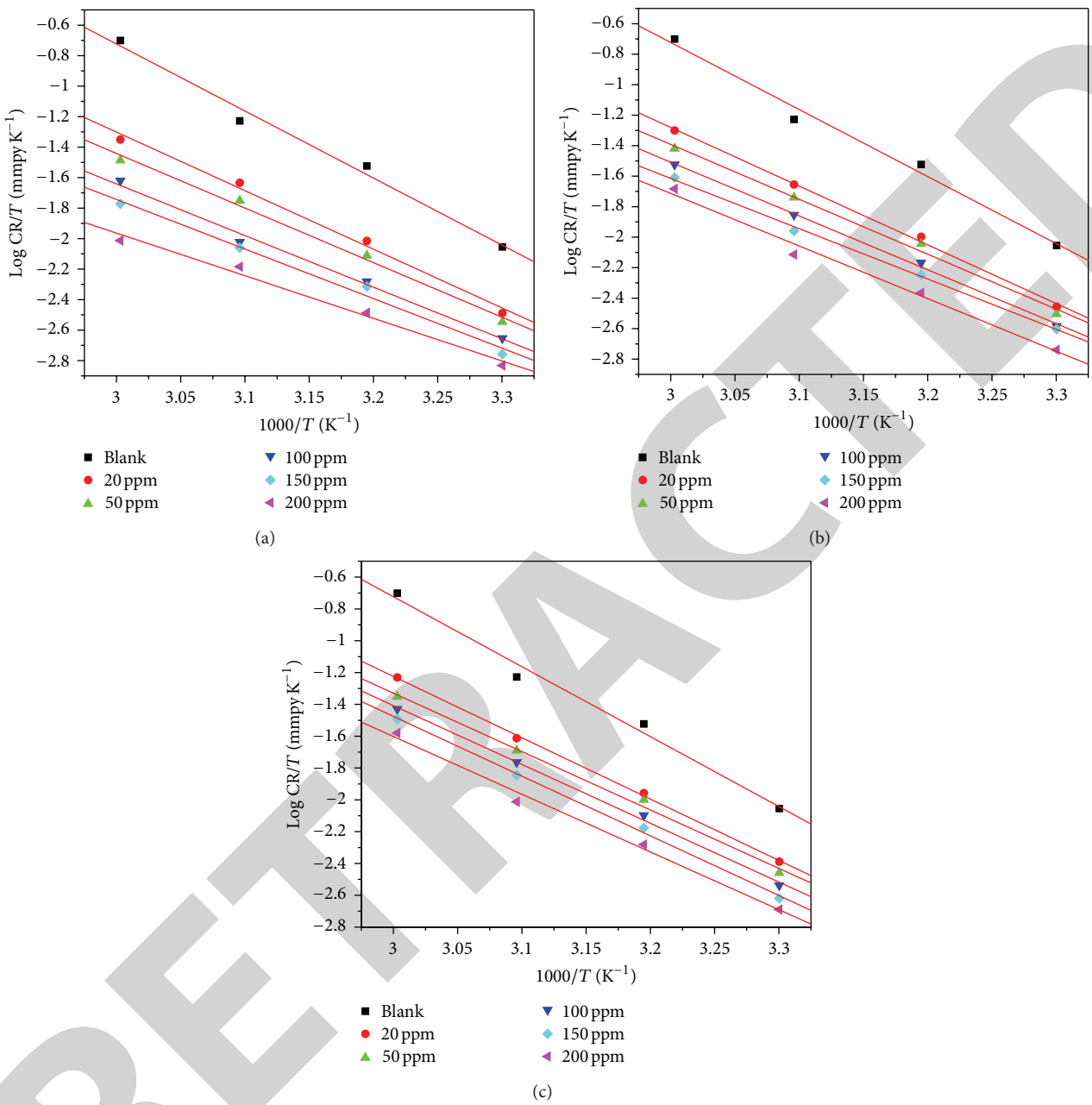

Figure 4: Transition state plot of log CR/T versus 1000/T for N80 steel in 15% HCl at different concentrations of (a) AMPT, (b) APT, and (c) ACPT.

where Y_0 is a proportionality factor and "n" has the meaning of phase shift. The value of "n" represents the deviation from the ideal behavior and it lies between 0 and 1.

The charge transfer resistance (R_{ct}), double-layer capacitance (C_{dl}) obtained from the Nyquist plots, and the calculated inhibition efficiency values (IE%) are shown in Table 7. It is clear that the value of R_{ct} increases with increasing the concentration of the inhibitor, indicating that the corrosion rate decreases in the presence of the inhibitor [34]. It is also clear that the value of C_{dl} decreases on the addition of inhibitors, indicating a decrease in the local dielectric constant and/or an increase in the thickness of the electrical double layer, suggesting that the inhibitor molecules function by the formation of the protective layer at the metal surface [35]. So, the changes in R_{ct} and C_{dl} values were caused by the steady replacement of the water molecules by the adsorption of inhibitor on mild steel surface, reducing the extent of dissolution [36]. The maximum inhibition efficiency was obtained for AMPT at 200 ppm concentration. Both electrochemical methods (polarization measurement and EIS study) offered nearly the same trend.

3.4. Adsorption Isotherm. Basic information on the interaction between the organic inhibitors and the N80 steel

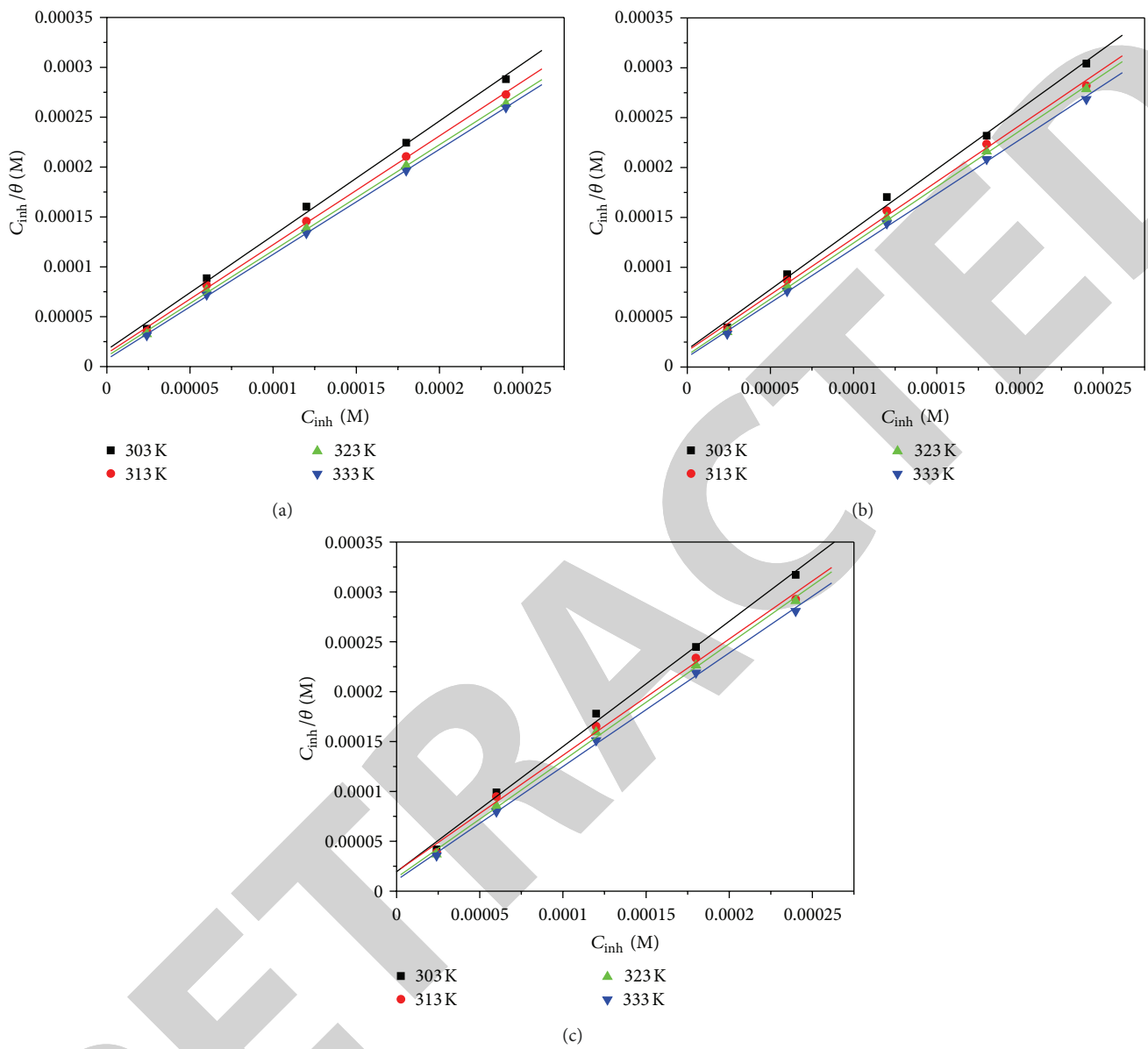

Figure 5: Langmuir plots of (C_{inh}/θ) versus C_{inh} for (a) AMPT, (b) APT, and (c) ACPT.

surface is obtained from various isotherms. Adsorption of these organic inhibitors has displaced the water molecule from the metal surface. The most commonly used adsorption isotherms are Langmuir, Temkin, and Frumkin. By far, the best fit was obtained with the Langmuir adsorption isotherm. The degree of surface coverage (θ) for different concentrations of inhibitor in 15% hydrochloric acid has been evaluated by the weight loss value. According to the Langmuir adsorption isotherm, the surface coverage (θ) is related to the inhibition concentration by the following equation:

$$\frac{C_{inh}}{\theta} = \frac{1}{K_{ads}} + C_{inh}, \tag{9}$$

where C_{inh} is the inhibitor concentration and K_{ads} is the equilibrium constant for adsorption-desorption process.

A plot of (C_{inh}/θ) versus C_{inh} (Figure 5) gives a straight line with an average correlation coefficient (R^2), ($R^2 = 0.998$, 0.997, and 0.999) for AMPT, APT, and ACPT, respectively, at 303 K which suggests that the adsorption obeys Langmuir adsorption isotherm. From the intercept, K_{ads} is calculated, and by using the value of K_{ads} the value of ΔG^0_{ads} was calculate by the following equation:

$$\Delta G^0_{ads} = -RT \ln\left(55.5 K_{ads}\right), \tag{10}$$

where R is the gas constant and T is the absolute temperature (K). The value of 55.5 is the molar concentration of water in solution in mol L^{-1}. In the present study a large value of K_{ads} was found for all the three studied inhibitors indicating the strong adsorption of inhibitor molecules at the surface of N80 steel. The values of ΔG^0_{ads} were −37.5, −35.2, and

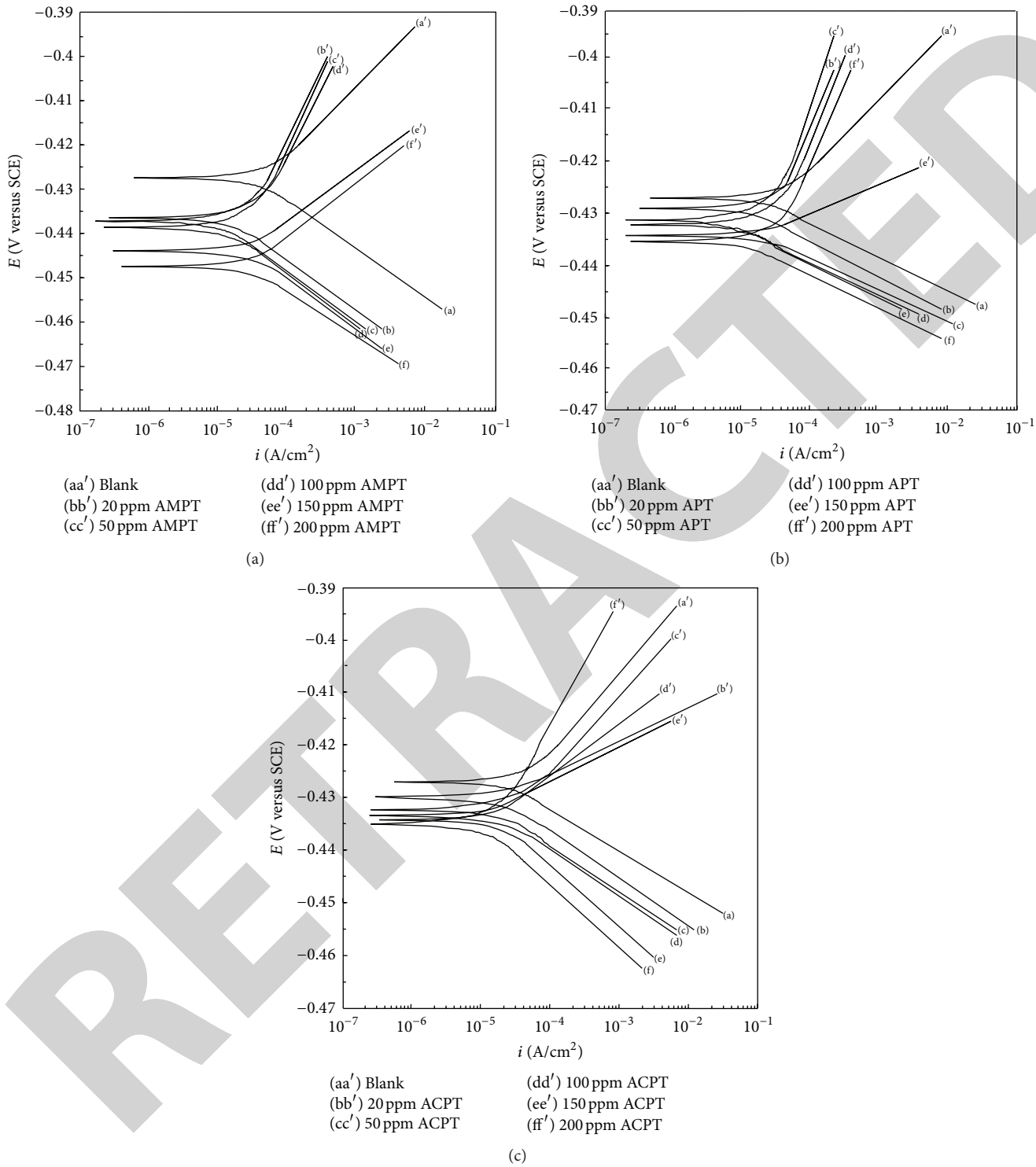

Figure 6: Potentiodynamic polarization curves for N80 steel in 15% HCl in the presence and the absence of inhibitors at 303 K. (a) AMPT, (b) APT, and (c) ACPT.

−32.1 kJ/mol for AMPT, APT, and ACPT, respectively. The negative values of ΔG^0_{ads} indicate a spontaneous adsorption process and stability of the adsorbed film of (AMPT, APT, and ACPT) on N80 surface [37]. It is generally accepted that for the values of ΔG^0_{ads} up to −20 kJ/mol, the types of adsorption were regarded as physisorption; the inhibition acts due to the electrostatic interactions between the charged molecules and the charged metallic surfaces, while the values around −40 kJ/mol or smaller were seen as chemisorption, which is due to the charge sharing or a transfer from the

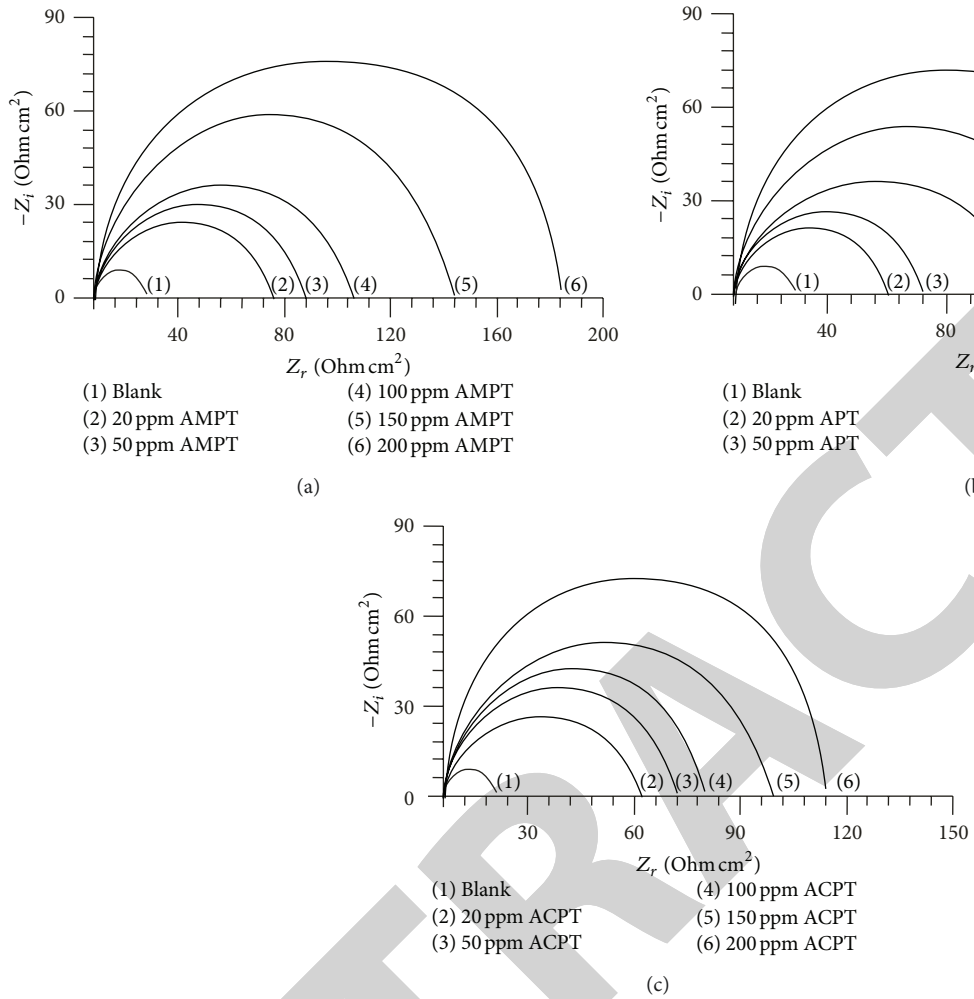

Figure 7: Nyquist plot for N80 steel in 15% HCl acid containing various concentrations of (a) AMPT, (b) APT, and (c) ACPT. (1) 0 ppm (2) 50 ppm (3) 100 ppm (4) 150 ppm, and (5) 200 ppm at 303 K.

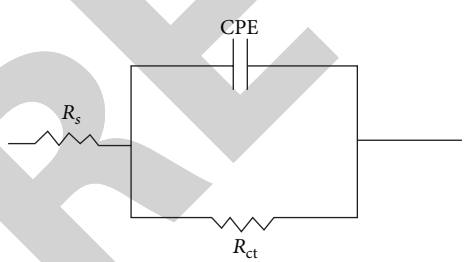

Figure 8: The electrochemical equivalent circuit used to fit the impedance measurements.

inhibitor's molecules to the metal surface to form a covalent bond [38, 39]. The values of ΔG^0_{ads} in our measurements range from −30 to −40 kJ·mol^{-1}; it is suggested that the adsorption of these molecules involves chemisorption.

The inhibition efficiency afforded by all the three inhibitors may be attributed to the presence of electron rich (N, S) atoms and delocalized π electrons. The possible coordinating centres are unshared electron pair of nitrogen of $-NH_2$ group, nitrogen of thiadiazole ring, C=N group, and π-electrons of phenyl and thiadiazole rings. The participation of phenyl ring during the adsorption of the inhibitors may be shown by higher % IE value in case of methoxy substituents having +I effect and lower values for chlorosubstituent with −I effect.

3.5. Scanning Electron Microscopy (SEM). The surface morphology of mild steel specimens exposed to 15% HCl solutions in the absence and presence of 200 ppm of AMPT are shown in Figures 9(a), 9(b), and 9(c). Figure 9(a) shows SEM image of polished bare N80 steel surface. Figure 9(b) reveals that the surface is severely corroded, and there is formation of different forms of corrosion products (iron oxides) on the surface in the absence of the inhibitor, and the entire surface is covered by a scale-like black corrosion product. The morphological feature of the inhibited surface with the addition of 200 ppm of AMPT is shown in Figure 9(c). On comparing these micrographs, it appears, that in the presence of inhibitors, the surface of the test material has improved remarkably with respect to its smoothness. The smoothening

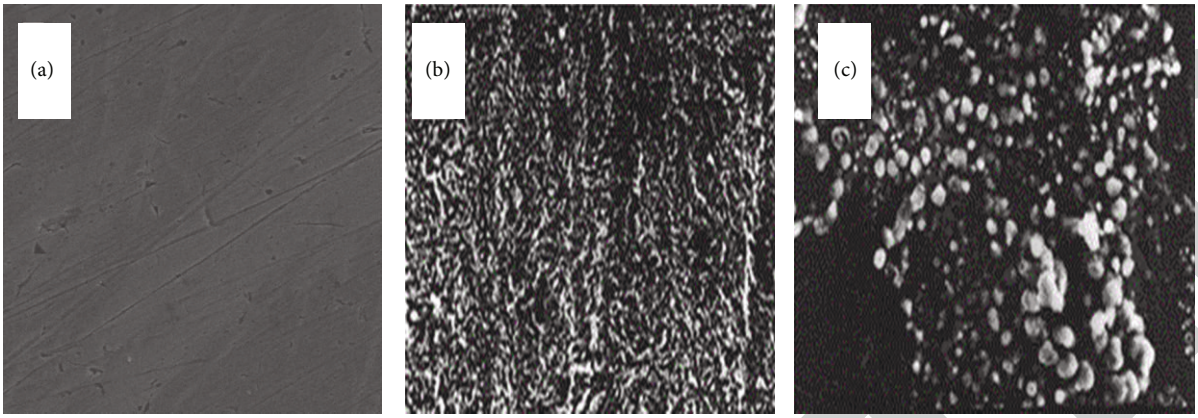

Figure 9: SEM image of N80 steel in 4 N HCl solution after 6 h immersion at 303 K (a) before immersion (polished) and (b) after immersion without inhibitor and (c) with inhibitor (AMPT).

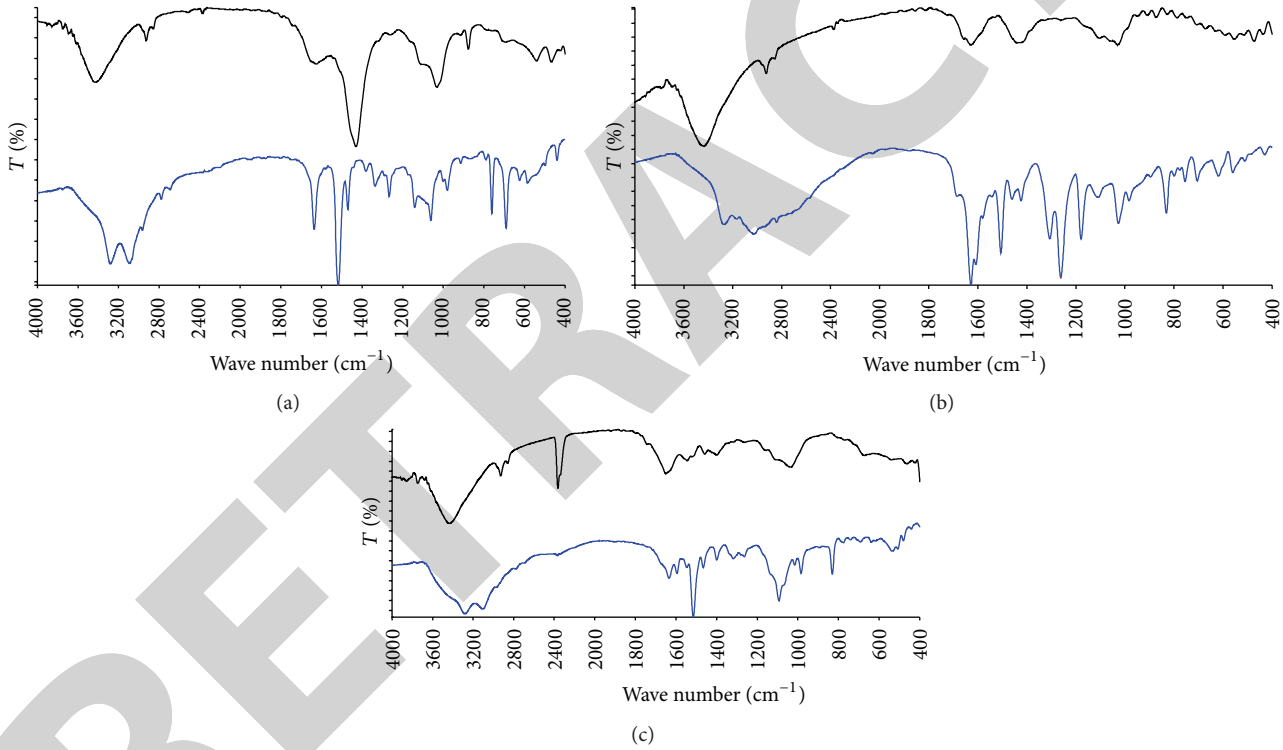

Figure 10: FTIR spectrum of the inhibitor (below), FT-IR spectrum of inhibitor adsorbed on metal surface (above). (a) AMPT, (b) APT, and (c) ACPT.

of the surface would have been caused by the adsorption of inhibitor molecules on it. But the closer look at such sites reveals that the inhomogeneities are due to the structural defects of the metal substrate and that these sites are also covered by the inhibitor film. This observation also accounts for the high inhibition efficiency values obtained during the weight loss studies of the inhibitor system.

3.6. FTIR Spectroscopic Analysis of Corrosion Product. The FTIR spectra of pure inhibitors and the surface films formed on N80 steel coupons immersed in 15% HCl containing optimum concentration of inhibitors (AMPT, APT, and ACPT) for 6 h are presented in Figures 10(a), 10(b), and 10(c). The FTIR spectra of pure AMPT show band at 3290 cm^{-1}, 3135 cm^{-1}, APT at 3355, 3160 cm^{-1} and ACPT at 3280, 3120 cm^{-1}, which indicate the asymmetrical and symmetrical N–H stretching vibrations for the amino group. Bands at 3280 cm^{-1}, 3125 cm^{-1} for AMPT, 3345, 3148 cm^{-1} for APT, and 3272, 3113 cm^{-1} for ACPT, respectively indicate the asymmetrical and symmetrical N–H stretching vibration for amino group. Strong peaks observed at 1640, 1630, and 1635 cm^{-1} are attributed to the N–H in plane bending

Table 7: Electrochemical impedance parameters and percentage inhibition efficiency for N80 steel in 15% HCl in the absence and the presence of the inhibitors at different concentrations at 303 K.

Inhibitor	Concentration (ppm)	R_{ct} ($\Omega\,cm^2$)	C_{dl} ($\mu F\,cm^2$)	% IE
Blank	—	25	252	
AMPT	20	74	158	66.32
	50	85	122	70.58
	100	110	87	77.25
	150	142	73	82.37
	200	178	67	85.97
APT	20	66	82	62.42
	50	75	66	67.71
	100	102	53	75.47
	150	126	32	80.13
	200	150	26	83.31
ACPT	20	63	71	60.52
	50	74	58	66.12
	100	80	41	68.58
	150	107	24	76.53
	200	134	20	81.03

vibrations of the amino group in pure AMPT, APT, and ACPT, respectively. Strong peaks observed at 1626, 1622, and 1620 cm^{-1} are attributed to the N–H in plane bending vibrations of the amino group in AMPT, APT, and ACPT, respectively. Strong bands at 1530, 1520, and 1525 cm^{-1} are attributed to the stretching vibration of the C=N group in the ring in pure AMPT, APT, and ACPT, respectively. Strong bands at 1523, 1512, and 1514 cm^{-1} are attributed to the stretching vibration of the C=N group in the ring in surface product of AMPT, APT, ACPT respectively. Peaks observed at 695, 690, and 680 cm^{-1} are attributed to the ring C–S vibration for pur AMPT, APT, and ACPT, respectively. Peaks observed at 690, 684, and 670 cm^{-1} are attributed to the ring C–S vibration for surface product of AMPT, APT, ACPT respectively. The presence of all the functional groups present in pure AMPT, APT, and ACPT in the spectrum of the surface product with a negative shift indicates the adsorption of inhibitors AMPT, APT, and ACPT at the surface of N80 steel.

4. Conclusions

(1) The synthesized thiadiazoles show good inhibition efficiencies for the corrosion of N80 steel in 15 wt% HCl solutions and the inhibition efficiency increases with increasing the concentration of these inhibitors and with the temperature. The increasing order of inhibiting performance of the inhibitors is in the order of: AMPT > APT > ACPT.

(2) Thiadiazoles inhibitors were found to be mixed-type inhibitors from Tafel polarization measurements. While one equivalent structure model was selected to fit the experimental data of the impedance diagram (EIS). And the results are good in agreement with weight loss measurements.

(3) It is suggested from the results obtained from Langmuir adsorption isotherm that the mechanism of corrosion inhibition is occurring mainly through adsorption process.

(4) Surface morphological studies such as FTIR and SEM analysis showed that a film of inhibitor is formed on the electrode surface.

Acknowledgment

One of the authors, Sumit Kumar, gratefully acknowledges Council for Scientific and Industrial Research (CSIR), New Delhi India, for research fellowship.

References

[1] I. Ahamad and M. A. Quraishi, "Bis (benzimidazol-2-yl) disulphide: an efficient water soluble inhibitor for corrosion of mild steel in acid media," *Corrosion Science*, vol. 51, no. 9, pp. 2006–2013, 2009.

[2] Q. B. Zhang and Y. X. Hua, "Corrosion inhibition of mild steel by alkylimidazolium ionic liquids in hydrochloric acid," *Electrochimica Acta*, vol. 54, no. 6, pp. 1881–1887, 2009.

[3] W. Li, Q. He, C. Pei, and B. Hou, "Experimental and theoretical investigation of the adsorption behaviour of new triazole derivatives as inhibitors for mild steel corrosion in acid media," *Electrochimica Acta*, vol. 52, no. 22, pp. 6386–6394, 2007.

[4] R. Solmaz, G. Kardas, B. Yazıcı, and M. Erbil, "Inhibition effect of rhodanine for corrosion of mild steel in hydrochloric acid solution," *Protection of Metals*, vol. 41, no. 6, pp. 581–585, 2005.

[5] G. Kardas, "The inhibition effect of 2-thiobarbituric acid on the corrosion performance of mild steel in HCl solution," *Fiziko-Khimicheskaya Mekhanika Materialov*, vol. 41, no. 3, pp. 337–343, 2005.

[6] M. Yadav, D. Behera, and U. Sharma, "Development of corrosion inhibitors used in acidization of petroleum oil well," *Der Chemica Sinica*, vol. 3, pp. 262–268, 2012.

[7] M. Yadav, D. Behera, and U. Sharma, "Nontoxic corrosion inhibitors for N80 steel in hydrochloric acid," *Arabian Journal of Chemistry*, 2012.

[8] M. A. Amin, S. S. Abd El-Rehim, E. E. F. El-Sherbini, and R. S. Bayoumi, "The inhibition of low carbon steel corrosion in hydrochloric acid solutions by succinic acid. Part I. Weight loss, polarization, EIS, PZC, EDX and SEM studies," *Electrochimica Acta*, vol. 52, no. 11, pp. 3588–3600, 2007.

[9] S. T. Selvi, V. Raman, and N. Rajendran, "Corrosion inhibition of mild steel by benzotriazole derivatives in acidic medium," *Journal of Applied Electrochemistry*, vol. 33, no. 12, pp. 1175–1182, 2003.

[10] F. Bentiss, M. Lebrini, H. Vezin, and M. Lagrenée, "Experimental and theoretical study of 3-pyridyl-substituted 1,2,4-thiadiazole and 1,3,4-thiadiazole as corrosion inhibitors of mild steel in acidic media," *Materials Chemistry and Physics*, vol. 87, no. 1, pp. 18–23, 2004.

[11] S. K. Shukla and E. E. Ebenso, "Effect of condensation product of thiosemicarbazide and phenyl isothiocynate on corrosion of

mild steel in sulphuric acid medium," *International Journal of Electrochemcal Science*, vol. 7, pp. 12134–12145, 2012.

[12] I. A. Ammar and S. Darwish, "Effect of some ions on inhibition of the acid corrosion of fe by thiourea," *Corrosion Science*, vol. 7, no. 9, pp. 579–596, 1967.

[13] D. D. N. Singh, M. M. Singh, R. S. Chaudhary, and C. V. Agarwal, "Inhibitive effects of isatin, thiosemicarbazide and isatin-3-(3-thiosemicarbazone) on the corrosion of aluminium alloys in nitric acid," *Journal of Applied Electrochemistry*, vol. 10, no. 5, pp. 587–592, 1980.

[14] G. Trabanelli, G. Brunoro, C. Monticells, and M. Foganolo, in *Proceedings of the 9th ICMC*, Toronto, Canada, June 1984.

[15] G. D. M. Z. Zhon, R. Tong, and T. Notoxa, *Bulletin of the Electrochemical Society*, vol. 7, p. 60, 1991.

[16] R. M. Souto, V. Fox, M. M. Laz, M. Pérez, and R. S. González, "Some experiments regarding the corrosion inhibition of copper by benzotriazole and potassium ethyl xanthate," *Journal of Electroanalytical Chemistry*, vol. 411, no. 1-2, pp. 161–165, 1996.

[17] E. Otero and J. M. Bastidas, "Cleaning of two hundred year-old copper works of art using citric acid with and without benzotriazole and 2-amino-5-mercapto-1,3,4-thiadiazole," *Materials and Corrosion*, vol. 47, no. 3, pp. 133–138, 1996.

[18] S. S. Mahmoud and E. G. A. Malidy, *Egyptian Journal of Chemistry*, vol. 39, p. 365, 1996.

[19] O. O. Xometl, N. V. Likhanova, N. Nava et al., "Thiadiazoles as corrosion inhibitors for carbon steel in H_2SO_4 solutions," *International Journal of Electrochemcal Science*, vol. 8, pp. 735–752, 2013.

[20] X. J. Raj and N. Rajendran, "Corrosion inhibition effect of substituted thiadiazoles on brass," *International Journal of Electrochemical Science*, vol. 6, no. 2, pp. 348–366, 2011.

[21] A. Shafiee, E. Naimi, P. Mansobi, A. Foroumadi, and M. Shekari, "Syntheses of substituted-oxazolo-1,3,4-thiadiazoles, 1,3,4-oxadiazoles, and 1,2,4-triazoles," *Journal of Heterocyclic Chemistry*, vol. 32, no. 4, pp. 1235–1239, 1995.

[22] N. A. Negm, A. A. Hafiz, and M. Y. El Awady, "Influence of structure of the cationic polytriethanolammonium bromide derivatives. II. Corrosion inhibition," *Egyptian Journal of Chemistry*, vol. 48, no. 2, pp. 201–210, 2005.

[23] A. U. Ezeoke, O. G. Adeyemi, O. A. Akerele, and N. O. Obi-Egbedi, "Computational and experimental studies of 4-Aminoantipyrine as corrosion inhibitor for mild steel in sulphuric acid solution," *International Journal of Electrochemical Science*, vol. 7, no. 1, pp. 534–553, 2012.

[24] E. E. Ebenso and I. B. Obot, "Inhibitive properties, thermodynamic characterization and quantum chemical studies of secnidazole on mild steel corrosion in acidic medium," *International Journal of Electrochemical Science*, vol. 5, no. 12, pp. 2012–2035, 2010.

[25] K. Jüttner, "Electrochemical impedance spectroscopy (EIS) of corrosion processes on inhomogeneous surfaces," *Electrochimica Acta*, vol. 35, no. 10, pp. 1501–1508, 1990.

[26] I. Dehri and M. Özcan, "The effect of temperature on the corrosion of mild steel in acidic media in the presence of some sulphur-containing organic compounds," *Materials Chemistry and Physics*, vol. 98, no. 2-3, pp. 316–323, 2006.

[27] G. Moretti, G. Quartarone, A. Tassan, and A. Zingales, "Pitting corrosion behavior of superferritic stainless steel in waters containing chloride," *Werkstoffe und Korrosion*, vol. 44, no. 1, pp. 24–30, 1993.

[28] V. R. Saliyan and A. V. Adhikari, "Inhibition of corrosion of mild steel in acid media by N'-benzylidene-3- (quinolin-4-ylthio)propanohydrazide," *Bulletin of Materials Science*, vol. 31, no. 4, pp. 699–711, 2008.

[29] D. Jayaperumal, "Effects of alcohol-based inhibitors on corrosion of mild steel in hydrochloric acid," *Materials Chemistry and Physics*, vol. 119, no. 3, pp. 478–484, 2010.

[30] W. H. Li, Q. He, S. T. Zhang, C. L. Pei, and B. R. Hou, "Some new triazole derivatives as inhibitors for mild steel corrosion in acidic medium," *Journal of Applied Electrochemistry*, vol. 38, no. 3, pp. 289–295, 2008.

[31] M. S. Morad, "An electrochemical study on the inhibiting action of some organic phosphonium compounds on the corrosion of mild steel in aerated acid solutions," *Corrosion Science*, vol. 42, no. 8, pp. 1307–1326, 2000.

[32] G. Gunasekaran and L. R. Chauhan, "Eco friendly inhibitor for corrosion inhibition of mild steel in phosphoric acid medium," *Electrochimica Acta*, vol. 49, no. 25, pp. 4387–4395, 2004.

[33] A. Alagta, I. Felhösi, J. Telegdi, I. Bertóti, and E. Kálmán, "Effect of metal ions on corrosion inhibition of pimeloyl-1,5-dihydroxamic acid for steel in neutral solution," *Corrosion Science*, vol. 49, no. 6, pp. 2754–2766, 2007.

[34] R. Solmaz, "Investigation of the inhibition effect of 5-((E)-4-phenylbuta-1,3-dienylideneamino)-1,3,4-thiadiazole-2-thiol Schiff base on mild steel corrosion in hydrochloric acid," *Corrosion Science*, vol. 52, no. 10, pp. 3321–3330, 2010.

[35] I. Ahamad, R. Prasad, and M. A. Quraishi, "Adsorption and inhibitive properties of some new Mannich bases of Isatin derivatives on corrosion of mild steel in acidic media," *Corrosion Science*, vol. 52, no. 4, pp. 1472–1481, 2010.

[36] B. Trachli, M. Keddam, H. Takenouti, and A. Srhiri, "Protective effect of electropolymerized 3-amino 1,2,4-triazole towards corrosion of copper in 0.5 M NaCl," *Corrosion Science*, vol. 44, no. 5, pp. 997–1008, 2002.

[37] J. D. Talati and D. K. Gandhi, "N-heterocyclic compounds as corrosion inhibitors for aluminium-copper alloy in hydrochloric acid," *Corrosion Science*, vol. 23, no. 12, pp. 1315–1332, 1983.

[38] Z. Szklarska-Smialowska and J. Mankowski, "Crevice corrosion of stainless steels in sodium chloride solution," *Corrosion Science*, vol. 18, no. 11, pp. 953–960, 1978.

[39] A. Yurt, S. Ulutas, and H. Dal, "Electrochemical and theoretical investigation on the corrosion of aluminium in acidic solution containing some Schiff bases," *Applied Surface Science*, vol. 253, no. 2, pp. 919–925, 2006.